

Single-diffractive production of dijets within the k_t -factorization approach

Marta Łuszczak,^{1,*} Rafał Maciuła,^{2,†} Antoni Szczurek^{c,2,§} and Izabela Babiarcz^{1,¶}

¹*Faculty of Mathematics and Natural Sciences,
University of Rzeszów, PL-35-959 Rzeszów, Poland*

²*Institute of Nuclear Physics PAN, PL-31-342 Cracow, Poland*

(Dated: March 1, 2022)

Abstract

We discuss single-diffractive production of dijets. The cross section is calculated within the resolved pomeron picture, for the first time in the k_t -factorization approach, neglecting transverse momentum of the pomeron. We use Kimber-Martin-Ryskin unintegrated parton (gluon, quark, antiquark) distributions (UPDF) both in the proton as well as in the pomeron or subleading reggeon. The UPDFs are calculated based on conventional MMHT2014nlo PDFs in the proton and H1 collaboration diffractive PDFs used previously in the analysis of diffractive structure function and dijets at HERA. For comparison we present results of calculations performed within collinear-factorization approach. Our results remained those obtained in the NLO approach. The calculation is (must be) supplemented by the so-called gap survival factor which may, in general, depend on kinematical variables. We try to describe the existing data from Tevatron and make detailed predictions for possible LHC measurements. Several differential distributions are calculated. The \bar{E}_T , $\bar{\eta}$ and $x_{\bar{p}}$ distributions are compared with the Tevatron data. A reasonable agreement is obtained for the first two distributions. The last one requires to introduce a gap survival factor which depends on kinematical variables. We discuss how the phenomenological dependence on one kinematical variable may influence dependence on other variables such as \bar{E}_T and $\bar{\eta}$. Several distributions for the LHC are shown.

PACS numbers: 13.87.Ce,12.38.Bx

^c also at University of Rzeszów, PL-35-959 Rzeszów, Poland

^{*} luszczak@ur.edu.pl

[†] rafal.maciula@ifj.edu.pl

[§] antoni.szczurek@ifj.edu.pl

[¶] i.babiarz@gmail.com

I. INTRODUCTION

The hard diffractive processes are related to the production of a system with large mass (gauge boson, Higgs boson), or large invariant mass (dijets), and a presence of a rapidity gap somewhere in rapidity space. Several hard diffractive processes were studied in the past. The gap may be in different places with respect to final state objects, e.g. between forwardly produced proton and a hard system (hard single diffractive process) or between jets (jet-gap-jet topology) or quarkonia (quarkonium-gap-quarkonium). Another category are exclusive diffractive processes (Higgs, dijets, $\gamma\gamma$, pair of heavy quarks $Q\bar{Q}$, etc.) Several other processes are possible in general, many of them not studied so far.

In the present paper we discuss single-diffractive production of dijets. This process was discussed in the past for photo- and electro-production [1–4] as well as for proton-proton or proton-antiproton collisions [5–9]. The hard single diffractive processes are treated usually in the resolved pomeron picture with a pomeron being a virtual but composed (of partons) object. This picture was used with a success for the description of hard diffractive processes studied extensively at HERA. This picture was tried to be used also at hadronic collisions. A few processes were studied experimentally at the Tevatron [10–20] including the dijet production.

The related calculation were performed so far in the context of collinear-factorization approach. The corresponding parton distributions in pomeron, or equivalently so-called diffractive parton distributions in the proton, were fitted so far to the HERA data. The distributions should be universal so, in principle, can be used in proton-proton collisions. In pp or $p\bar{p}$ collisions the strong nonperturbative interactions can easily destroy the rapidity gap associated with pomeron (or other color-singlet) exchange. This effect is of nonperturbative nature and therefore difficult to be controlled. There were several attempts to understand the related suppression of the hard diffractive cross sections. Usually the effect is quantified by a phenomenological gap survival factor. The factor is known to be energy dependent because the nonperturbative soft interactions are known to be energy dependent. In general, the survival probability may depend on other kinematical variables. Recently the gap survival factor was studied for jet-gap-jet processes [21] and the dependence on the gap sizes was discussed in the picture of multiple parton scattering.

In our opinion we are still far from the full understanding of the dynamical effect.

In the present paper we intend to treat the single-diffractive dijet production for the first time within the k_t -factorization approach. Similar approach was used recently for the single-diffractive production of $c\bar{c}$ pairs [22]. The k_t -factorization approach was also used recently for non-diffractive dijet [23], three- [24] or even four-jet production [25]. In particular, we wish to compare results obtained within collinear-factorization and k_t -factorization approaches. A comparison with the Tevatron data is planned. We would like to make also predictions for the LHC.

II. A SKETCH OF THE APPROACH

In this paper we follow the theoretical framework proposed very recently by three of us in Ref. [22]. There, some new ideas for calculation of diffractive cross sections were put forward and applied in the case of single-diffractive production of charm at the LHC. According to this approach, the standard resolved pomeron model [26], usually based on the leading-order (LO) collinear approximation, is extended by adopting a framework of the k_t -factorization as an effective way to include higher-order corrections. It was shown several times, that the k_t -factorization approach is very useful in this context and especially efficient in the studies of kinematical correlations (see *e.g.* Refs. [23, 27]).

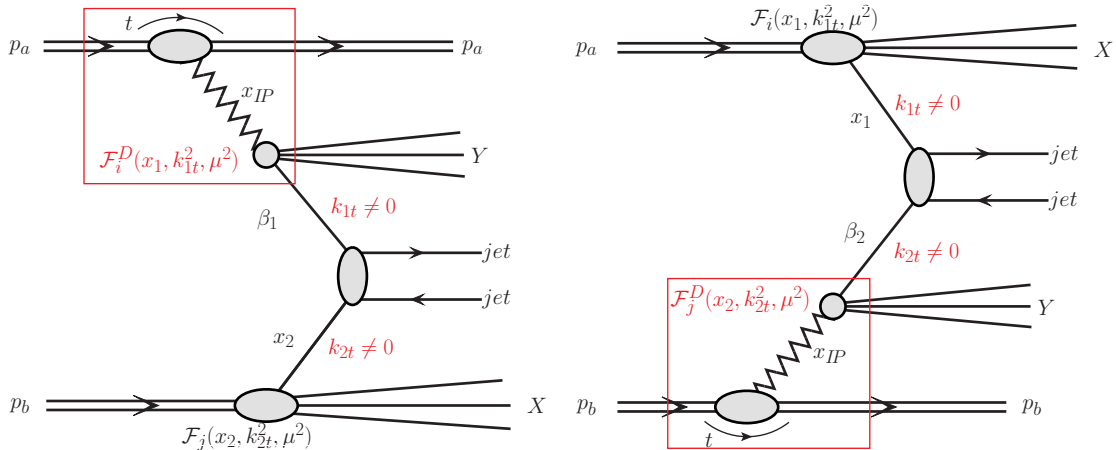


FIG. 1. A diagrammatic representation of the considered mechanisms of single-diffractive dijet production within resolved pomeron model extended in the present paper to the k_t -factorization approach.

A sketch of the mechanisms under consideration, relevant for the inclusive single-

diffractive production of dijets in pp or $p\bar{p}$ collisions, with the notation of kinematical variables and with some theoretical ingredients used in the following is shown in Fig. 1.

According to the approach introduced above, the cross section for inclusive single-diffractive production of dijet, for both considered diagrams (left and right panel of Fig. 1), can be written as:

$$d\sigma^{SD(1)}(p_a p_b \rightarrow p_a \text{ dijet } XY) = \sum_{i,j,k,l} \int dx_1 \frac{d^2 k_{1t}}{\pi} dx_2 \frac{d^2 k_{2t}}{\pi} d\hat{\sigma}(i^* j^* \rightarrow kl) \\ \times \mathcal{F}_i^D(x_1, k_{1t}^2, \mu^2) \cdot \mathcal{F}_j(x_2, k_{2t}^2, \mu^2), \quad (2.1)$$

$$d\sigma^{SD(2)}(p_a p_b \rightarrow \text{dijet } p_b XY) = \sum_{i,j,k,l} \int dx_1 \frac{d^2 k_{1t}}{\pi} dx_2 \frac{d^2 k_{2t}}{\pi} d\hat{\sigma}(i^* j^* \rightarrow kl) \\ \times \mathcal{F}_i(x_1, k_{1t}^2, \mu^2) \cdot \mathcal{F}_j^D(x_2, k_{2t}^2, \mu^2), \quad (2.2)$$

where $\mathcal{F}_i(x, k_t^2, \mu^2)$ are the "conventional" unintegrated (k_t -dependent) parton distributions (UPDFs) in the proton and $\mathcal{F}_i^D(x, k_t^2, \mu^2)$ are their diffractive counterparts – which we will call here diffractive UPDFs (dUPDFs). The latter can be interpreted as a probability of finding a parton i with longitudinal momentum fraction x and transverse momentum (virtuality) k_t at the factorization scale μ^2 assuming that the proton which lost a momentum fraction x_{IP} remains intact.

The $2 \rightarrow 2$ partonic cross sections in Eqs.(2.1) and (2.2) read:

$$d\hat{\sigma}(i^* j^* \rightarrow kl) = \frac{d^3 p_1}{2E_1(2\pi)^3} \frac{d^3 p_2}{2E_2(2\pi)^3} (2\pi)^2 \delta^2(p_1 + p_2 - k_1 - k_2) \times \overline{|\mathcal{M}_{i^* j^* \rightarrow kl}(k_1, k_2)|^2} \quad (2.3)$$

with $i, j, k, l = g, u, d, s, \bar{u}, \bar{d}, \bar{s}$, where p_1, E_1 and p_2, E_2 are the momenta and energies of outgoing partons, respectively, and $\mathcal{M}_{i^* j^* \rightarrow kl}(k_1, k_2)$ are the off-shell matrix elements for the $i^* j^* \rightarrow kl$ subprocesses with initial state partons i and j being off mass shell. In the numerical calculations here we include all $2 \rightarrow 2$ partonic channels:

$$\begin{aligned} \#1 &= g^* g^* \rightarrow gg, & \#4 &= g^* g^* \rightarrow q\bar{q}, & \#7 &= q^* \bar{q}^* \rightarrow gg, \\ \#2 &= q^* g^* \rightarrow qg, & \#5 &= q^* \bar{q}^* \rightarrow q\bar{q}, & \#8 &= q^* q^* \rightarrow qq, \\ \#3 &= g^* q^* \rightarrow gq, & \#6 &= q^* \bar{q}^* \rightarrow q' \bar{q}', & \#9 &= q^* q'^* \rightarrow qq'. \end{aligned}$$

The relevant gauge-invariant off-shell matrix elements for each of the channels above can be calculated *e.g.* within the method of parton reggeization. It was done recently in Ref. [23] where the matrix elements were presented in a very useful analytical form.

As we have proposed very recently in Ref. [22], the diffractive UPDFs can be calculated using their collinear counterparts via the Kimber-Martin-Ryskin (KMR) method [28, 29]. Then, the diffractive unintegrated parton distributions for gluon and quark are given by the following formulas:

$$f_g^D(x, k_t^2, \mu^2) \equiv \frac{\partial}{\partial \log k_t^2} \left[g^D(x, k_t^2) T_g(k_t^2, \mu^2) \right] = T_g(k_t^2, \mu^2) \frac{\alpha_S(k_t^2)}{2\pi} \times \int_x^1 dz \left[\sum_q P_{gq}(z) \frac{x}{z} q^D\left(\frac{x}{z}, k_t^2\right) + P_{gg}(z) \frac{x}{z} g^D\left(\frac{x}{z}, k_t^2\right) \Theta(\Delta - z) \right], \quad (2.4)$$

$$f_q^D(x, k_t^2, \mu^2) \equiv \frac{\partial}{\partial \log k_t^2} \left[q^D(x, k_t^2) T_q(k_t^2, \mu^2) \right] = T_q(k_t^2, \mu^2) \frac{\alpha_S(k_t^2)}{2\pi} \times \int_x^1 dz \left[P_{qq}(z) \frac{x}{z} q^D\left(\frac{x}{z}, k_t^2\right) \Theta(\Delta - z) + P_{qg}(z) \frac{x}{z} g^D\left(\frac{x}{z}, k_t^2\right) \right], \quad (2.5)$$

where g^D and q^D are the collinear diffractive PDFs in the proton. The P_{qq} , P_{qg} , P_{gq} and P_{gg} are the usual unregulated LO DGLAP splitting functions and T_g and T_q are the gluon and quark Sudakov form factors, respectively. More details of the whole procedure and discussion of all of the ingredients can be found *e.g.* in Ref. [29].

According to the so-called proton-vertex-factorization, the diffractive collinear PDF in the proton, *e.g.* for gluon, has the following generic form:

$$g^D(x, \mu^2) = \int dx_{IP} d\beta \delta(x - x_{IP}\beta) g_{IP}(\beta, \mu^2) f_{IP}(x_{IP}) = \int_x^{x^{max}} \frac{dx_{IP}}{x_{IP}} f_{IP}(x_{IP}) g_{IP}\left(\frac{x}{x_{IP}}, \mu^2\right), \quad (2.6)$$

where $\beta = \frac{x}{x_{IP}}$ is the longitudinal momentum fraction of the pomeron carried by gluon and the flux of pomerons may be taken as:

$$f_{IP}(x_{IP}) = \int_{t_{min}}^{t_{max}} dt f(x_{IP}, t). \quad (2.7)$$

An analogous expression can be also written for the collinear diffractive quark distribution.

In this paper, the diffractive KMR UPDFs are calculated from the "H1 2006 fit A" diffractive collinear PDFs [30], that are only available at next-to-leading order (NLO). In the calculation of the conventional non-diffractive KMR UPDFs the collinear MMHT2014nlo PDFs [31] were used. In the perturbative part of calculations we take running coupling constant $\alpha_S(\mu_R^2)$ and the renormalization and factorization scales equal to $\mu^2 = \mu_R^2 = \mu_F^2 = \frac{p_{1t}^2 + p_{2t}^2}{2}$, where p_{1t} and p_{2t} are the transverse momenta of the outgoing jets.

III. RESULTS

In this section we shall show results of our calculations. We shall start from a trial of the description of the Tevatron experimental data [13, 14].

A. Tevatron cuts

We start from showing our results for $\bar{E}_T = \frac{E_{1T} + E_{2T}}{2}$ and $\bar{\eta} = \frac{\eta_1 + \eta_2}{2}$ distributions, see Fig. 2. In this calculation the pomeron/reggeon longitudinal momentum fraction was limited as in experimental case [13, 14] to $0.035 < x_{IP,IR} < 0.095$. We show both naive result obtained with the KMR UGDF (dashed line) as well as similar results with limitations on parton transverse momenta $k_T < p_T^{sub}$ (solid line) and $k_T < 7$ TeV (dash-dotted line). The first limitation was proposed for standard nondiffractive jets [23]. The latter limitation is related to the lower experimental cut on jet transverse momenta. For comparison we show also distribution obtained in leading-order collinear factorization approach (dotted line). A large difference can be seen close to the lower transverse momentum cut. Similar effect was discussed recently for four jet production in [25].

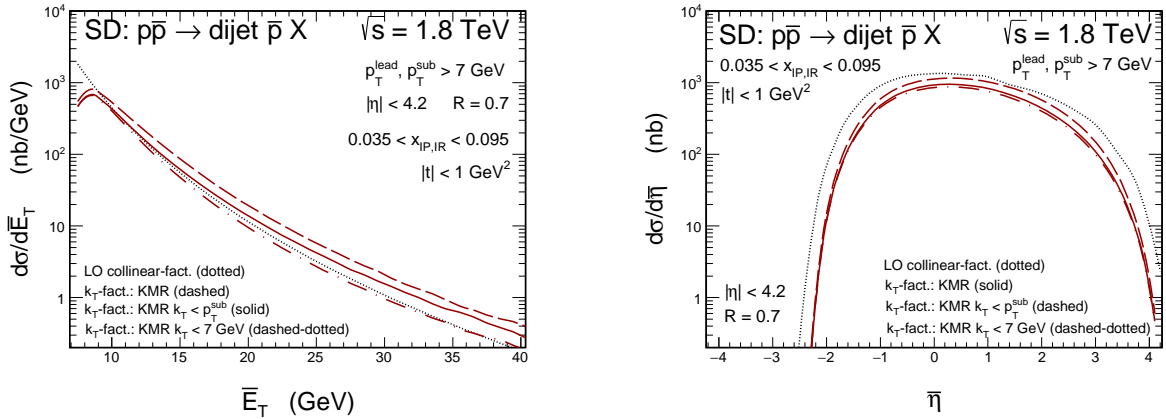


FIG. 2. Distribution in average \bar{E}_T (left panel) and in average $\bar{\eta}$ (right panel). Here $S_G = 0.1$.

Fig. 3 shows somewhat theoretical two-dimensional distribution in transverse momenta of partons. Surprisingly the distribution is almost symmetric in k_{1T} and k_{2T} . The limitation on parton transverse momenta $k_T < p_T^{sub}$ makes the two-dimensional distribution much narrower, although the consequences on distribution in transverse momenta and rapidity are not dramatic as has been already shown in Fig. 2.

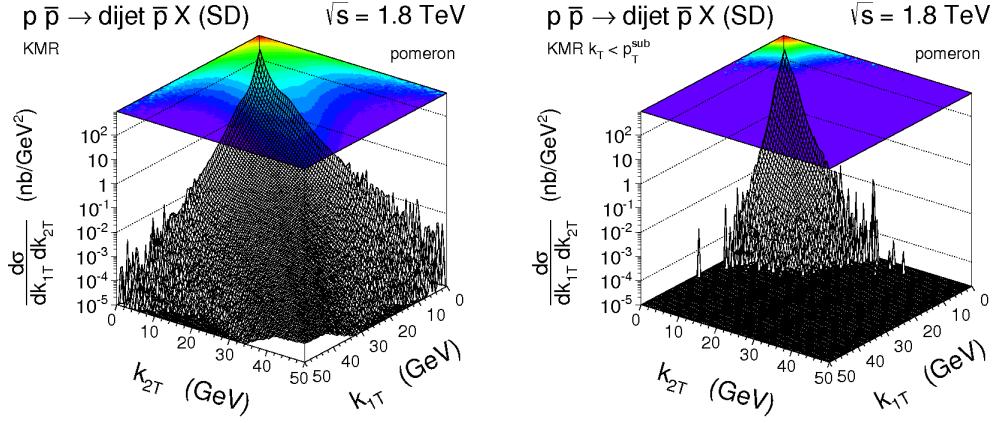


FIG. 3. Two dimensional distribution in transverse momenta of partons on the nondiffractive side (k_{1T}) and on the diffractive side (k_{2T}). Here $S_G = 0.1$.

In contrast to the leading-order collinear factorization approach, in the k_t -factorization approach the transverse momentum distribution of leading (solid) and subleading (dashed) jets differ as is shown in the left panel of Fig. 4

Here a standard cut on parton transverse momentum has been imposed. The single diffractive cross section depends on the cut on four-momentum squared transferred to the outgoing antiproton (antiproton was measured in the CDF experiment). The cut changes the cross section normalization but does not modify the shape of the distribution.

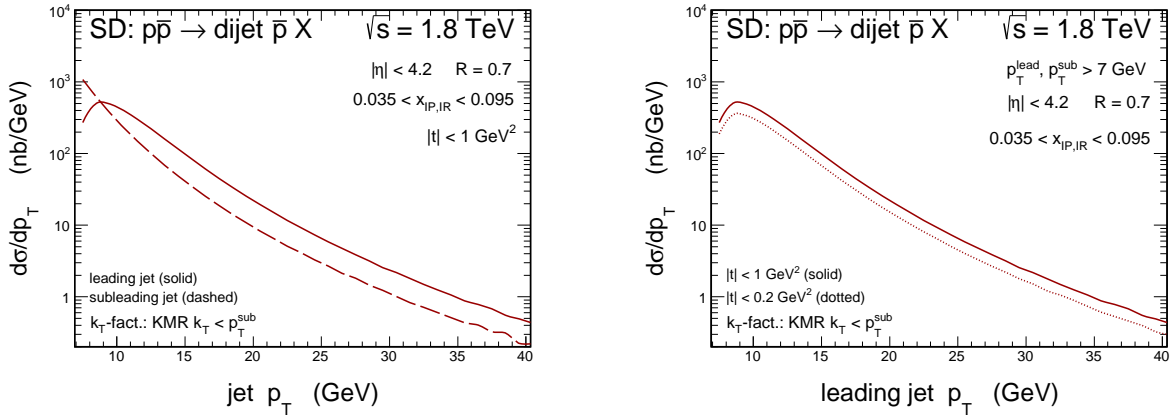


FIG. 4. Transverse momentum distribution for leading and subleading jet (left panel) and the influence of the cut on t on the leading jet (right panel). Here $S_G = 0.1$.

In our calculation we include both pomeron and subleading reggeon exchanges. In the selected range of x_{IP} the pomeron contribution is much bigger than the contribution

of the subleading reggeon as shown in Fig. 5. The subleading reggeon contribution is about 10 % of the single diffractive cross section. For the average jet rapidity distribution the situation is a bit more complicated. Both contributions are of the same order for large $\bar{\eta}$.

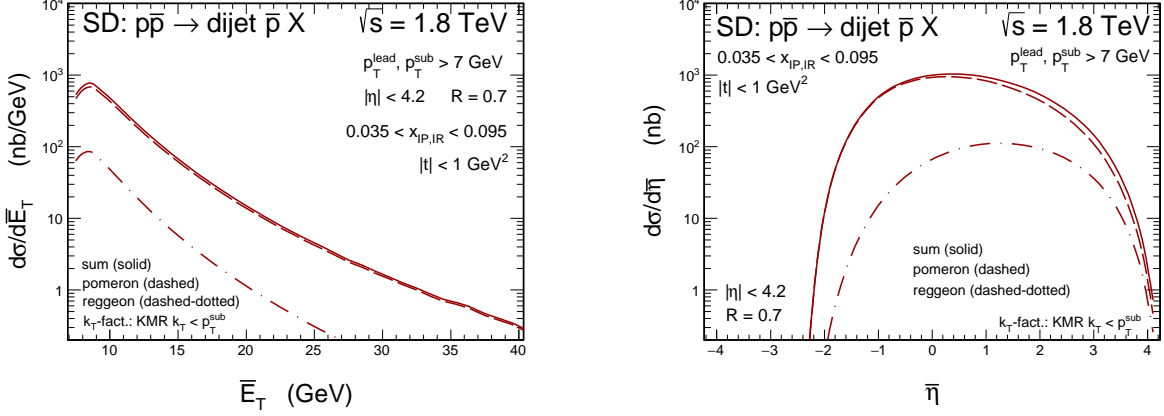


FIG. 5. The pomeron and subleading reggeon contribution for \bar{E}_T (left panel) and $\bar{\eta}$ (right panel).

Now we would like to consider distributions that can be compared to the experimental ones.

In Fig. 6 we show distribution in \bar{E}_T for two collision energies. While the k_t -factorization approach gives a better description of the data close to the lower experimental cut on jet transverse momenta, the collinear-factorization approach seems to be better for larger transverse momenta. This is true for both Tevatron collision energies. We do not have good understanding of the result.

In Fig. 7 we show distributions in average jet rapidity again for the two collision energies. Here the k_t -factorization result better describes the experimental data than the result obtained in the collinear approach. The outgoing antiproton is at $\eta \approx -6.05$ for $\sqrt{s} = 1.8$ TeV and $\eta \approx -5.53$ for $\sqrt{s} = 630$ GeV, respectively.

Let us note here that both the experimental distributions in \bar{E}_T and in $\bar{\eta}$ are not absolutely normalized (inspect description of "y" axes of Fig. 6 and Fig. 7). On the theoretical side the absolute cross section depends on gap survival factor which is not easy to calculate from first principle. The CDF collaboration showed also distribution in $x_{\bar{p}}$ normalized to the inclusive cross section. Our theoretical result is clearly above the experimental result, see Fig. 8. Roughly a factor of order 0.1 is missing in our calculation although the

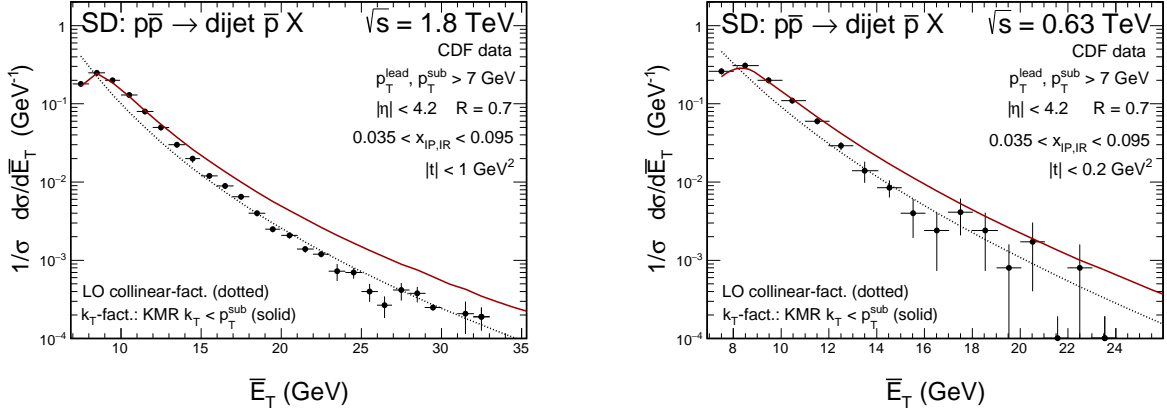


FIG. 6. The average transverse energy distribution for $\sqrt{s} = 1.8$ TeV (left panel) and for $\sqrt{s} = 630$ GeV (right panel).

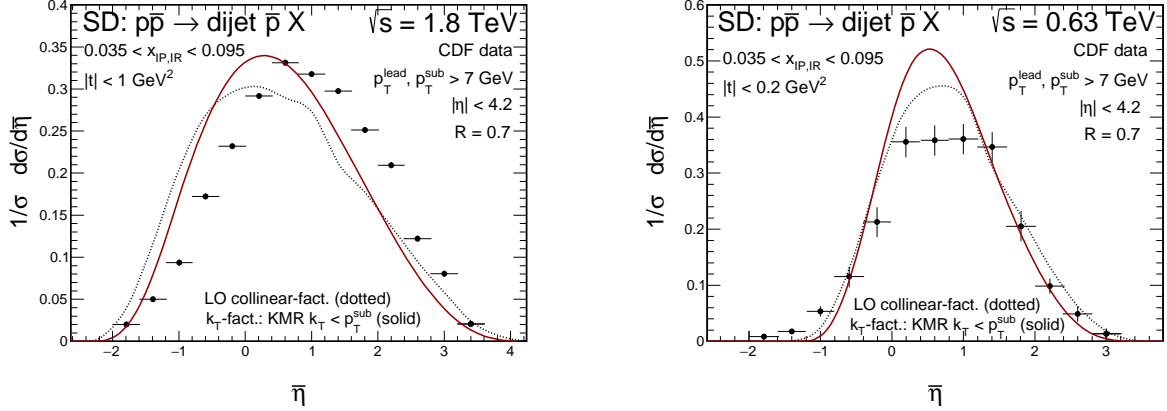


FIG. 7. The average rapidity distribution for $\sqrt{s} = 1.8$ TeV (left panel) and for $\sqrt{s} = 630$ GeV (right panel).

exact shape is not exactly the same.

There can be several reasons of the disagreement of our results with the CDF data. One of them is not a perfect extraction of the diffractive distributions at HERA. Another one is the dependence of the gap survival factor on kinematical variables. This possibility will be discussed now in the next subsection.

B. Kinematical dependence of gap survival factor

In this section we assume that the gap survival factor is a function of $x_{\bar{p}}$ only. This assumption is a bit academic but we would like to see a possible influence of such a

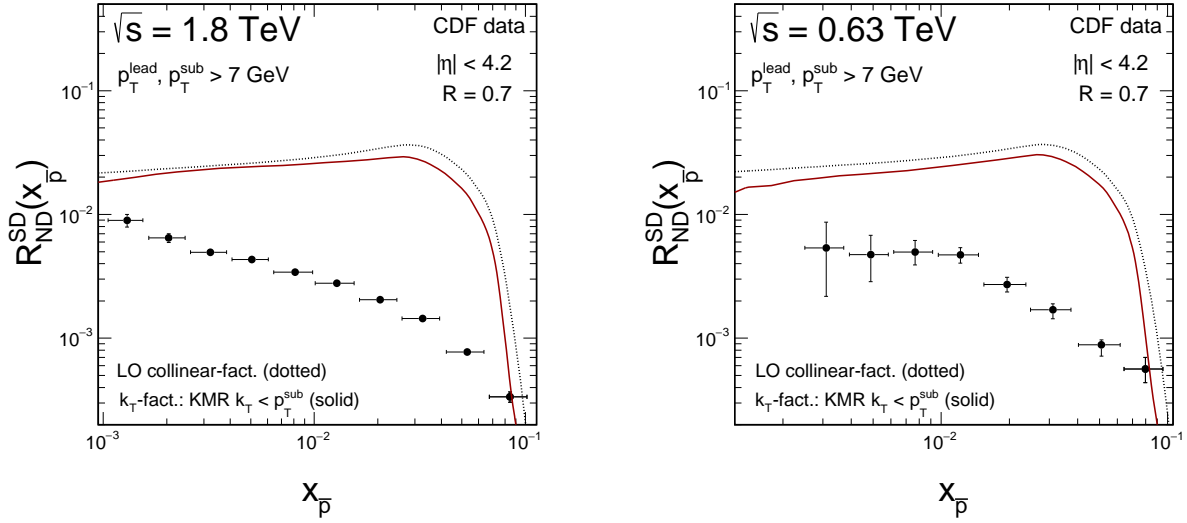


FIG. 8. Distribution in $x_{\bar{p}}$ for $\sqrt{s} = 1.8$ TeV (left panel) and for $\sqrt{s} = 630$ GeV (right panel). No gap survival factor was included here.

dependence on other distributions. In Fig. 9 we show a fit to the data assuming some functional form for $S_G(x_{\bar{p}})$, $S_G(x_{\bar{p}}) = 0.0056 * (x_1^{-0.6} + x_1^{-0.02})$ for collinear case and $S_G(x_{\bar{p}}) = 0.004 * (x_1^{-0.6} + x_1^{-0.03})$ for k_t -factorization approach. Our fit nicely describes the CDF data at $\sqrt{s} = 1.8$ TeV.

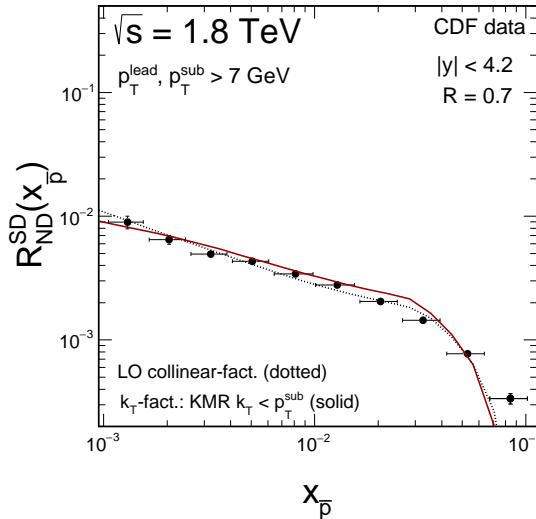


FIG. 9. The ratio of single-diffractive to nondiffractive cross sections as a function of $x_{\bar{p}}$. The lines are fits of S_G to the CDF data.

In Fig. 10 we again show distribution in \bar{E}_T for collinear (left panel) and k_t -factorization

(right panel) approaches. The inclusion of the dependence of S_G on $x_{\bar{p}}$ improves the overall agreement with the CDF data.

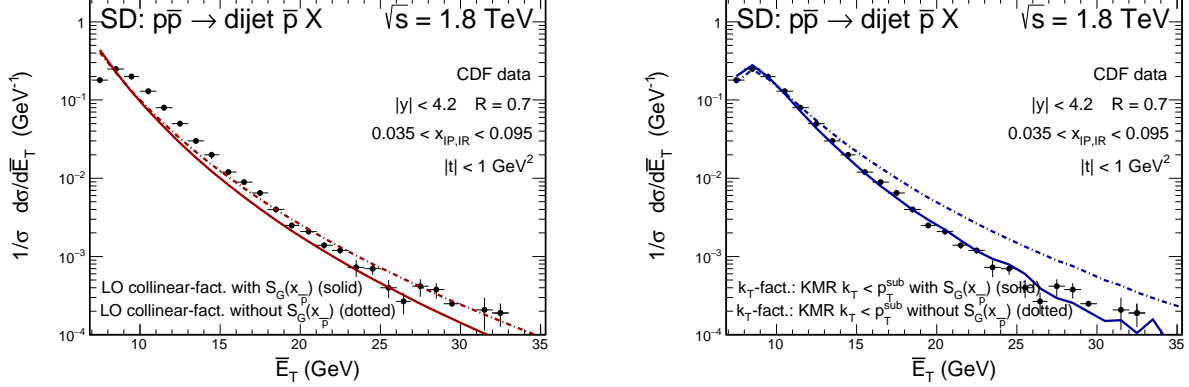


FIG. 10. \bar{E}_T distribution for collinear (left panel) and k_t -factorization (right panel) approaches with and without inclusion of the dependence of S_G on $x_{\bar{p}}$.

In Fig. 11 we show similar distributions in $\bar{\eta}$. One can observe a sizable shift of the distributions towards larger $\bar{\eta}$. The shift is in a correct direction but is much too big. This should be traced back to the extreme assumption of the dependence of S_G on $x_{\bar{p}}$ only. In reality S_G may depend on a few kinematical variables. However, such a study goes far beyond the scope of the present paper.

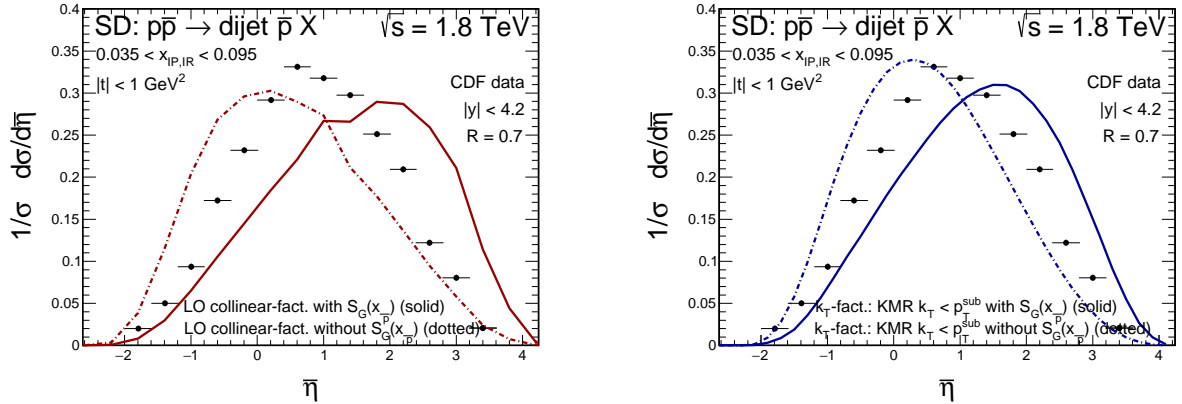


FIG. 11. $\bar{\eta}$ distribution for collinear (left panel) and k_t -factorization (right panel) approaches with and without inclusion of the dependence of S_G on $x_{\bar{p}}$.

C. Predictions for the LHC

In this subsection we would like to present our results for the LHC energy $\sqrt{s} = 13$ TeV. In our calculations we use cuts relevant for the planned ATLAS experiments, so we use range of rapidities relevant for the ATLAS experiment $-4.9 < y_1, y_2 < 4.9$. We consider rather low cut on the transverse momenta of jets $p_t > 20$ GeV. In the following we shall use $S_G = 0.05$.

In Fig. 12 we show distribution in jet transverse momentum, for leading (left panel) and subleading (right panel) jets. As for the Tevatron we discuss the role of extra cuts on parton transverse momenta. The cuts have bigger effect on leading jets.

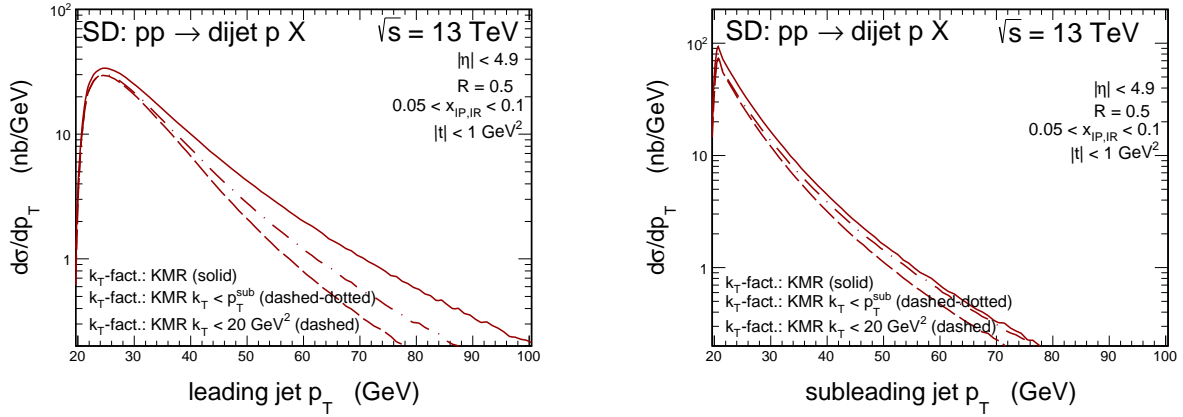


FIG. 12. Distribution in the jet transverse momentum for leading (left panel) and subleading (right panel) for $\sqrt{s} = 13$ TeV and for the ATLAS cuts. Here $S_G = 0.05$.

In Fig. 13 we compare contributions of the pomeron and subleading reggeon for the ATLAS range of $x_{IP,IR}$. The subleading contribution is larger than 10%. There is no evident dependence on the value of the transverse momentum.

In Fig. 14 we show similar distributions for jet rapidity again for leading and subleading jet. As previously we show contributions of pomeron and subleading reggeon separately. Here the relative contribution of subleading reggeon is an evident function of rapidity, both for leading and subleading jet.

Azimuthal angle correlations between the leading and subleading jet are shown in Fig. 15. Similar shapes are obtained for pomeron and reggeon contributions.

Finally in Fig. 16 we show purely theoretical two-dimensional distributions in transverse momenta of partons for pomeron (left panel) and subleading reggeon (right panel),

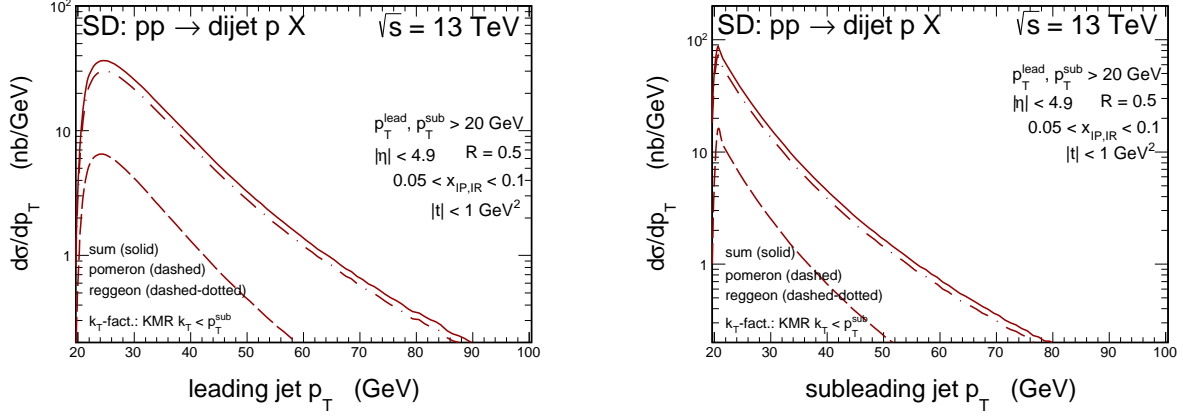


FIG. 13. The contribution of pomeron and subleading reggeon for transverse momentum distribution for leading (left panel) and subleading (right panel) jet for $\sqrt{s} = 13$ TeV and for the ATLAS cuts. Here $S_G = 0.05$.

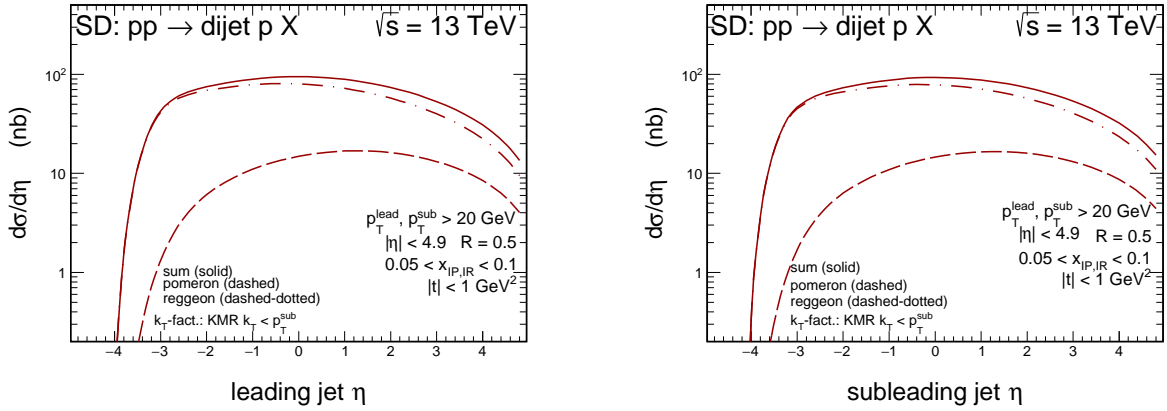


FIG. 14. Distribution in the jet rapidity for leading (left panel) and subleading (right jet) jet for $\sqrt{s} = 13$ TeV. Here $S_G = 0.05$.

respectively, for nondiffractive and diffractive sides. As for the Tevatron the distributions are surprisingly symmetric in k_{1T} and k_{2T} . In this calculation no extra cuts on parton transverse momenta have been imposed. We stress that very large transverse momenta of partons enter the considered dijet production.

In Table I we present the integrated cross section for the ATLAS acceptance for single-diffractive production of dijets for different cuts of the jet- p_T .

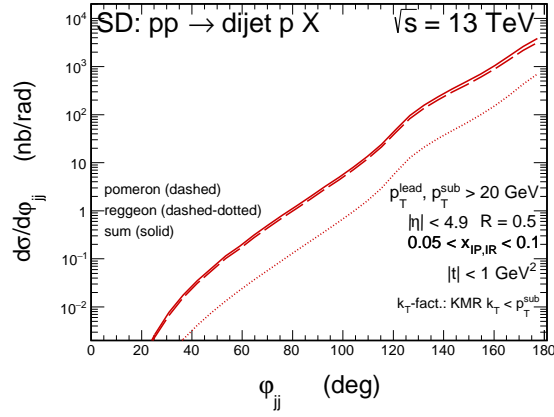


FIG. 15. Our predictions for azimuthal angle correlations between leading and subleading jet. Here $S_G = 0.05$.

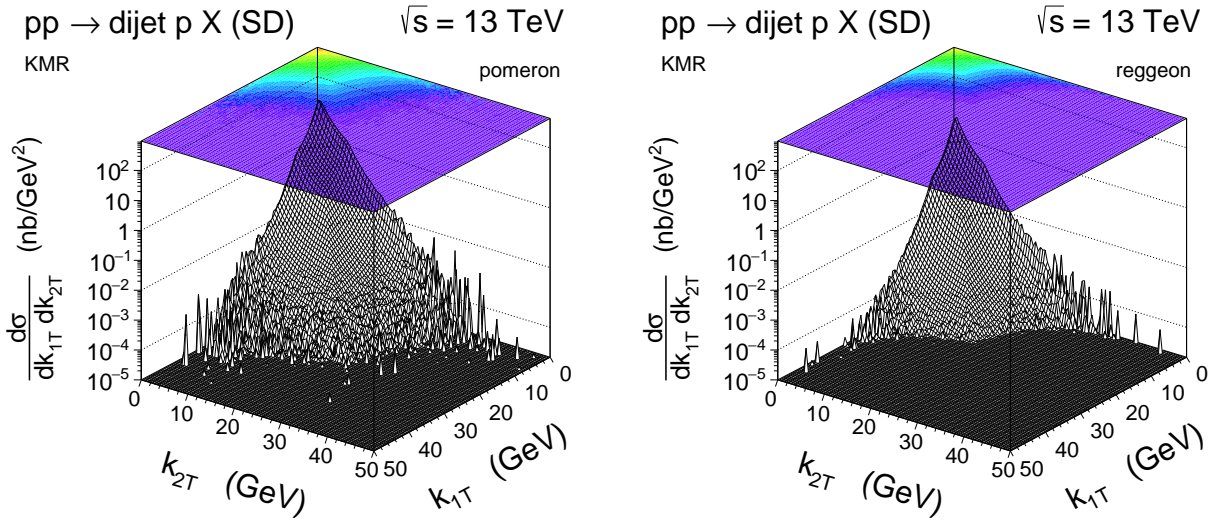


FIG. 16. Two-dimensional distributions in parton transverse momenta for pomeron (left panel) and subleading reggeon (right panel). In this calculation $\sqrt{s} = 13$ TeV and ATLAS cuts were imposed. Here $S_G = 0.05$.

TABLE I. The calculated cross sections in microbarns for single-diffractive production of dijets in pp -scattering at $\sqrt{s} = 13$ TeV for different cuts on transverse momentum of the dijets. Here, the rapidity of the dijets is $|y^{jet}| < 4.9$, that corresponds to the ATLAS detector acceptance. The cross section here is not multiplied by the gap survival factors.

$p_{T,min}^{jet}$ cuts	collinear		k_T -factorization approach	
	MMHT2014nlo	KMR	KMR $k_T < p_{T,min}^{jet}$ (IP)	KMR $k_T < p_{T,min}^{jet}$ (IR)
$p_T^{jet} > 20$ GeV	9.08	11.42	8.53	1.79
$p_T^{jet} > 35$ GeV	2.34	3.89	3.89	0.62
$p_T^{jet} > 50$ GeV	0.42	0.83	0.68	0.16

IV. CONCLUSIONS

In the present paper we have presented for the first time results for the single-diffractive production of dijets within k_t -factorization approach. The resolved pomeron model with flux of pomeron and reggeon and parton distribution in pomeron have been used. The diffractive unintegrated parton distributions were obtained based on their collinear counterparts. The latter were used to fit the HERA data for diffractive F_2 structure function and for diffractive dijet production. The rapidity gap is not calculated but can be fitted to the data. A constant value was assumed as a default.

Results of our calculations were compared with the Tevatron data where forward antiprotons and rapidity gaps were measured. We have calculated distributions in \bar{E}_T and $\bar{\eta}$. A reasonable agreement has been achieved. We have compared results obtained within collinear and k_t -factorization approaches. The k_t -factorization leads to a better description in E_T close to the lower transverse momentum cut.

Several other distributions have been presented and discussed, many of them for a first time.

It is rather difficult to describe the distributions in $x_{\bar{p}}$ with a constant value of gap survival factor, especially for $\sqrt{s} = 1.8$ TeV. We have considered a possibility that the gap survival factor depends exclusively on $x_{\bar{p}}$ and studied consequences for other observables. A phenomenological $x_{\bar{p}}$ function was used to fit the Tevatron data. Such a dependence of the gap survival factor leads to an effective shift of the distribution in $\bar{\eta}$ in better agreement with the Tevatron data. Our preliminary study suggest that the dependence of gap survival factor on kinematical variables can be also an important ingredient in order to understand details of rapidity distributions. Clearly further studies are necessary in a future.

We have also made predictions for future LHC measurements. Several differential distributions have been presented. We hope for their verification in a near future.

Acknowledgements

This study was partially supported by the Polish National Science Centre grants DEC-

- [1] M. Klasen and G. Kramer, *Eur. Phys. J. C* **38**, 93 (2004) [hep-ph/0408203].
- [2] A. B. Kaidalov, V. A. Khoze, A. D. Martin and M. G. Ryskin, *Eur. Phys. J. C* **66**, 373 (2010) [arXiv:0911.3716 [hep-ph]].
- [3] M. Klasen and G. Kramer, *Eur. Phys. J. C* **70**, 91 (2010) doi:10.1140/epjc/s10052-010-1436-x [arXiv:1006.4964 [hep-ph]].
- [4] V. Guzey and M. Klasen, *Eur. Phys. J. C* **76**, no. 8, 467 (2016) [arXiv:1606.01350 [hep-ph]].
- [5] R. B. Appleby and J. R. Forshaw, *Phys. Lett. B* **541**, 108 (2002) [hep-ph/0111077].
- [6] A. B. Kaidalov, V. A. Khoze, A. D. Martin and M. G. Ryskin, *Phys. Lett. B* **559**, 235 (2003) [hep-ph/0302091].
- [7] M. Klasen and G. Kramer, *Phys. Rev. D* **80**, 074006 (2009) [arXiv:0908.2531 [hep-ph]].
- [8] C. Royon, arXiv:1310.4675 [hep-ph].
- [9] C. Marquet, C. Royon, M. Saimpert and D. Werder, *Phys. Rev. D* **88**, no. 7, 074029 (2013).
- [10] F. Abe *et al.* [CDF Collaboration], *Phys. Rev. Lett.* **79**, 2636 (1997).
- [11] T. Affolder *et al.* [CDF Collaboration], *Phys. Rev. Lett.* **84**, 232 (2000).
- [12] T. Affolder *et al.* [CDF Collaboration], *Phys. Rev. Lett.* **85**, 4215 (2000).
- [13] T. Affolder *et al.* [CDF Collaboration], *Phys. Rev. Lett.* **84**, 5043 (2000).
- [14] D. Acosta *et al.* [CDF Collaboration], *Phys. Rev. Lett.* **88**, 151802 (2002).
- [15] M. H. L. S. Wang *et al.*, *Phys. Rev. Lett.* **87**, 082002 (2001).
- [16] T. Affolder *et al.* [CDF Collaboration], *Phys. Rev. Lett.* **87**, 241802 (2001).
- [17] T. Aaltonen *et al.* [CDF Collaboration], *Phys. Rev. Lett.* **99**, 242002 (2007).
- [18] T. Aaltonen *et al.* [CDF Collaboration], *Phys. Rev. D* **77**, 052004 (2008).
- [19] T. Aaltonen *et al.* [CDF Collaboration], *Phys. Rev. D* **82**, 112004 (2010).
- [20] T. Aaltonen *et al.* [CDF Collaboration], *Phys. Rev. Lett.* **108**, 081801 (2012).
- [21] I. Babiarz, R. Staszewski and A. Szczurek, arXiv:1704.00546 [hep-ph].
- [22] M. Luszczak, R. Maciula, A. Szczurek and M. Trzebinski, *JHEP* **1702**, 089 (2017) [arXiv:1606.06528 [hep-ph]].
- [23] M. A. Nefedov, V. A. Saleev and A. V. Shipilova, *Phys. Rev. D* **87**, no. 9, 094030 (2013).
- [24] A. van Hameren, P. Kotko and K. Kutak, *Phys. Rev. D* **88**, 094001 (2013) Erratum: [*Phys. Rev.*

- D **90**, no. 3, 039901 (2014)].
- [25] K. Kutak, R. Maciula, M. Serino, A. Szczurek and A. van Hameren, JHEP **1604**, 175 (2016) [arXiv:1602.06814 [hep-ph]].
- [26] G. Ingelman, P.E. Schlein, Phys. Lett. B **152**, 256 (1985).
- [27] R. Maciula and A. Szczurek, Phys. Rev. D **87**, no. 9, 094022 (2013).
- [28] M. A. Kimber, A. D. Martin and M. G. Ryskin, Phys. Rev. D **63**, 114027 (2001).
- [29] G. Watt, A. D. Martin and M. G. Ryskin, Phys. Rev. D **70** (2004) 014012 Erratum: [Phys. Rev. D **70** (2004) 079902].
- [30] A. Aktas *et al.* [H1 Collaboration], Eur. Phys. J. C **48**, 715 (2006).
- [31] L. A. Harland-Lang, A. D. Martin, P. Motylinski and R. S. Thorne, Eur. Phys. J. C **75**, no. 5, 204 (2015).